

# Intermittency in passive scalar turbulence under the uniform mean scalar gradient

Takeshi Watanabe<sup>a)</sup> and Toshiyuki Gotoh<sup>b)</sup>

Department of Engineering Physics, Graduate School of Engineering, Nagoya Institute of Technology, Gokiso, Showa-ku, Nagoya 466-8555, Japan

(Received 31 October 2005; accepted 28 April 2006; published online 22 May 2006)

Small scale statistics of a passive scalar convected by turbulence under the uniform mean scalar gradient is studied by high-resolution direct numerical simulation. It is found that the scaling exponents of the structure functions of scalar increments in parallel and perpendicular directions to the mean gradient are the same and saturate approximately 1.3 at large order, and that they are dependent on scalar injection scheme at large scales within the Reynolds numbers studied. Tails of the probability density functions for the scalar increment in the inertial convective range are well fitted by a scaling form inferred from the saturation and the tail of the one point scalar probability density function. © 2006 American Institute of Physics. [DOI: 10.1063/1.2206810]

Universality in turbulence has long been a central issue in fundamental physics of turbulence since Kolmogorov. The universality of the passive scalar turbulence means that when the velocity field at small scales is in an asymptotic statistical state which is independent of large scales, the passive scalar statistics becomes independent of the large scales of both scalar and velocity fields.<sup>1-3</sup> In the studies of the passive scalar turbulence the velocity is various, for example, homogeneous isotropic or sheared, or synthetic, and so on. Apart from the synthetic velocity case, the asymptotic states of both velocity and scalar are very difficult to attain experimentally or numerically, so that one has to carefully analyze and interpret the results of the experiments or direct numerical simulations (DNSs) with the consideration of the velocity statistics.<sup>4</sup>

To get more precise knowledge it is very effective to change large scale conditions of the scalar alone while keeping the turbulent velocity field the same and to see the difference in the scalar statistics. It is ideal for this purpose to choose the isotropic turbulent velocity having a well developed scaling range under the Navier-Stokes (NS) dynamics. The large scale condition of the passive scalar can be changed, for example, by using the random isotropic source or the uniform scalar gradients. The latter introduces the anisotropy to the scalar field. Celani *et al.* have studied the passive scalar in this direction in the energy inverse cascading range of the two-dimensional (2D) turbulence.<sup>5,6</sup> It was found that the scaling exponents were the same to the two kinds of the scalar sources and saturated at large order, but the anisotropy was persistent at small scales. Those facts are also consistent with the predictions of the Kraichnan model of the velocity scaling exponent  $0 < \xi < 2$  in any space dimensions, in spite of differences in the correlation time of the velocity, finite for the NS flow or delta correlated for the Kraichnan velocity.<sup>3,7-9</sup> This bears an expectation that the

scaling exponents of the passive scalar convected by the generic turbulent flow are universal.<sup>3,5,6,10,11</sup>

However, in the inverse cascading range of 2D turbulence the velocity statistics is so close to the Gaussian that the intermittency vanishes. On the other hand, in three dimensions (3D), the velocity is strongly intermittent and long lived structure of the velocity field leads to persistent correlation of the Lagrangian fluid particles. Moreover, recent study has shown that the transfer of the scalar variance to small scales is more efficient and more nonlocal than the case of the energy, suggesting sensitivity of the small scales of the passive scalar to the large scale conditions.<sup>12</sup> These facts raise possibility that the universality of the passive scalar is different from that suggested by 2D case and the Kraichnan model.

In order to get insight into this problem, we examine the passive scalar turbulence in 3D by using high resolution DNS. We use the statistically same isotropic steady turbulence with large scale random Gaussian forcing and the two kinds of scalar sources described in the following.

Governing equation of motion for a scalar field  $\theta(\mathbf{x}, t)$  is given by  $(\partial_t + u_j \partial_j) \theta = \kappa \partial_j^2 \theta + f_\theta$ , where an incompressible velocity field  $u_i(\mathbf{x}, t)$  obeys the NS equation  $(\partial_t + u_j \partial_j) u_i = -\partial_i P + \nu \partial_j^2 u_i + f_i$  with  $\partial_i u_i = 0$ . The coefficient  $\nu$  and  $\kappa$  are the kinematic viscosity and molecular diffusivity, respectively. Schmidt number  $Sc = \nu / \kappa$  is fixed to be unity throughout this Brief Communication. The random force  $f_i$  is solenoidal, Gaussian white in time and applied at low wave number band.<sup>13</sup> The isotropic source  $f_\theta$  is a random Gaussian white in time<sup>14</sup> (named by case *R*) or a uniform mean scalar gradient (case *G*),  $f_\theta = -Gu_3$ ,<sup>15</sup> where  $G$  is constant and fixed as  $G = 1$ . The detailed numerical scheme of DNS is the same as that in case *R*.<sup>14</sup> Here we mainly show the results at  $R_\lambda = 427$  (case *R*) and  $R_\lambda = 468$  (case *G*) with  $N^3 = 1024^3$  grid points. Statistical average in a steady state is taken over space and time during 4 (2.5) large eddy turnover times for case *G* (case *R*) and denoted by angular brackets. As far as the statistics in the convection dominated scaling range are

<sup>a)</sup>Electronic mail: watanabe@nitech.ac.jp

<sup>b)</sup>Electronic mail: gotoh.toshiyuki@nitech.ac.jp

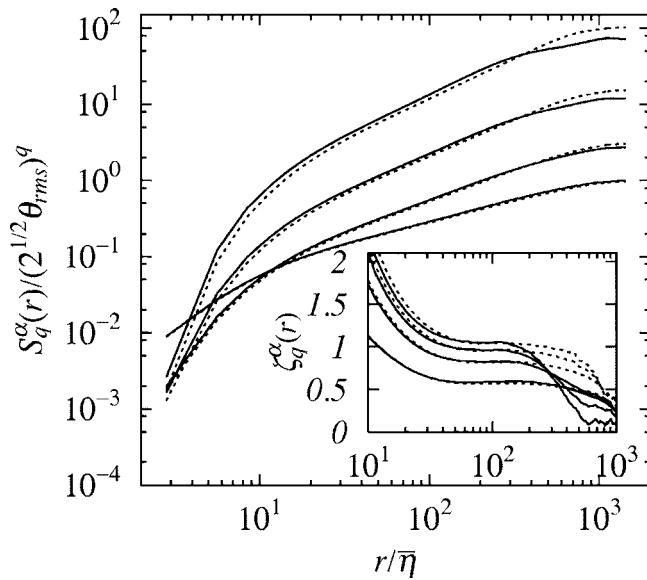


FIG. 1. The scalar structure functions for  $\delta_\parallel \theta$  (solid lines) and  $\delta_\perp \theta$  (dotted lines) normalized by  $(\sqrt{2} \theta_{rms})^q$  with  $q=2, 4, 6$ , and  $8$  from the lowermost curve. (Inset) Behavior of corresponding local scaling exponent  $\zeta_q^\alpha(r)$ .

concerned, the present DNS satisfies the accuracy conditions.<sup>16</sup>

The scalar structure function is defined by  $S_q^\alpha(r) = \langle (\delta_\alpha \theta_r)^q \rangle$ , where  $\delta_\alpha \theta_r \equiv \theta(\mathbf{x} + r\mathbf{e}_\alpha) - \theta(\mathbf{x})$  is a scalar increment and  $\mathbf{e}_\alpha$  is a unit vector in parallel ( $\alpha = \parallel$ ) and perpendicular ( $\alpha = \perp$ ) to the mean gradient. Figure 1 shows the variation of the even order structure functions as  $q=2m$  ( $m=1, \dots, 4$ ) to the separation distance  $r$  normalized by the Kolmogorov scale  $\bar{\eta}$ . Curves for  $S_{2m}^\parallel(r)$  and  $S_{2m}^\perp(r)$  up to  $m=2$  almost collapse, and those for high order are very close. The same is found for  $\langle |\delta_\alpha \theta_r|^{2m+1} \rangle$  (figure not shown).

Scaling behavior of  $S_q^\alpha(r)$  are examined by the local scaling exponent defined by  $\zeta_q^\alpha(r) \equiv d \log S_q^\alpha(r) / d \log r$ . Curves for  $\zeta_q^\alpha(r)$  are shown in the inset of Fig. 1. Although the width of plateau of the curves decreases with increase of  $q$ , we safely evaluate the exponents in the range  $60 < r/\bar{\eta} < 200$ , where the 4/3 law is observed (figure not shown).<sup>17</sup> Note that the plateau range of  $\delta_\perp \theta$  is wider than that of  $\delta_\parallel \theta$ .

In order to reduce the effect of anisotropy on the scaling behavior, we compute the structure functions  $S_q^G(r) = (S_q^\parallel(r) + 2S_q^\perp(r))/3$  in which the contributions from the sector of the angular momentum  $l=2$  are eliminated and higher contributions of  $l \geq 4$  are assumed to be very small,<sup>18</sup> i.e.,  $S_q^G(r)$  is predominated by an isotropic sector of  $S_q^\alpha(r)$ . Inset in Fig. 2 shows the variation of the local slope  $\zeta_q^G(r)$  of  $S_q^G(r)$ , where the result of case  $R$ <sup>14</sup> (denoted by  $\zeta_q^R(r)$ ) is also shown for comparison. There is no trend that there exist two scaling ranges, the inertial convective range (ICR) and the viscous-convective precursor range (VCPR) as found in case  $R$  (see Figs. 23 and 29 of Ref. 14 for details). Figure 2 shows the  $q$ th order scaling exponents evaluated by averaging the local slopes over  $r$  within the plateau range for case  $G$  ( $\zeta_q^\parallel$ ;  $60 \leq r/\bar{\eta} \leq 130$ ,  $\zeta_q^\perp$ , and  $\zeta_q^G$ ;  $60 \leq r/\bar{\eta} \leq 200$ ) and for case  $R$  ( $\zeta_q^R$  in ICR or VCPR).<sup>14</sup> The error bar of the scaling exponent was estimated by its mean error due to the temporal

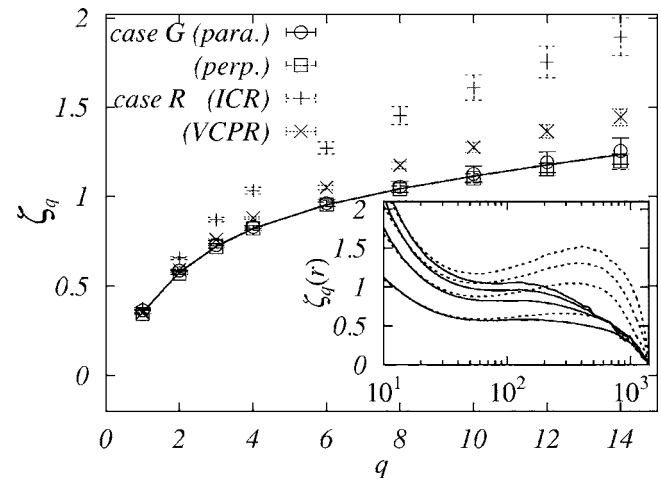


FIG. 2. The scaling exponents for case  $G$  (circles;  $\zeta_q^\parallel$ , squares;  $\zeta_q^\perp$ , solid line;  $\zeta_q^G$ ) and case  $R$  (plus signs;  $\zeta_q^R$  in ICR, crosses;  $\zeta_q^R$  in VCPR). Values of  $\zeta_q^G$  with  $q=2m$ , ( $m=1, \dots, 7$ ) are  $0.578 \pm 0.003$ ,  $0.822 \pm 0.008$ ,  $0.95 \pm 0.01$ ,  $1.04 \pm 0.02$ ,  $1.11 \pm 0.03$ ,  $1.18 \pm 0.04$ , and  $1.24 \pm 0.05$ . Values of  $\zeta_q^R$  can be found in Ref. 14. (Inset) Behavior of local scaling exponent for case  $G$  ( $\zeta_q^G(r)$ ; solid line) and case  $R$  ( $\zeta_q^R(r)$ ; dotted line) against  $r/\bar{\eta}$ . Order  $q=2m$  is  $m=1, \dots, 4$  from the lowermost curve.

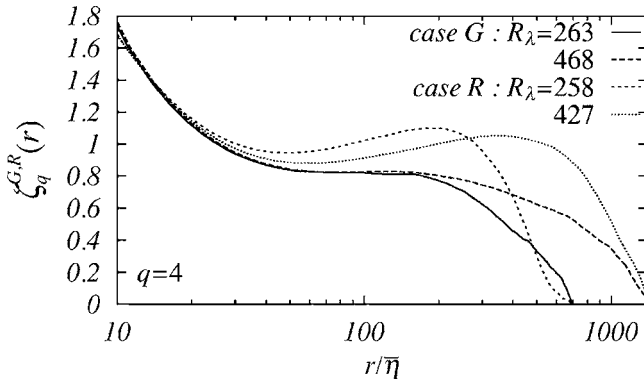
fluctuations over the duration of the time average, and found to be small enough to discuss the difference. Points of Figs. 1 and 2 are:

- (i) Same scaling exponents as  $\zeta_q^\parallel \approx \zeta_q^\perp \approx \zeta_q^G$  for even orders up to  $q=14$  in the range  $60 \leq r/\bar{\eta} \leq 130$ .
- (ii) In the scaling range of  $60 \leq r/\bar{\eta} \leq 200$ ,  $\zeta_q^G(r)$  tends to saturate at high order as  $\zeta_\infty^G(r) \approx 1.3$  and the difference  $\zeta_q^R(r) - \zeta_q^G(r) (> 0)$  becomes larger as  $q$  increases.

As for the observation (i), Gylfason and Warhaft<sup>4</sup> experimentally observed  $\zeta_q^\parallel \approx \zeta_q^\perp$  in the grid turbulence, which is consistent with our observation. However the values of the scaling exponents are larger than those by the present case  $G$ , i.e., the scalar in the present DNS is more intermittent than that in their experiments.

Now the observation (ii). Results of Fig. 2 are contrast to those by Celani *et al.*,<sup>5,6</sup> in which they observed the same behavior of the local scaling exponents irrespective of cases  $G$  or  $R$  in the energy inverse cascading range in 2D, and both of which saturate at about  $\zeta_\infty^{G,R} \approx 1.4$ . If we restrict ourselves to the scaling behavior in VCPR of  $30 < r/\bar{\eta} < 60$ , the curves  $\zeta_q^G(r)$  are close to those of  $\zeta_q^R(r)$  up to  $q=4$ , whereas the differences are beyond the error bars for  $q > 4$ . On the other hand, in the range of  $60 < r/\bar{\eta} < 200$ , the curves  $\zeta_q^G(r)$  stay on the same values as those in VCPR, and become appreciably below  $\zeta_q^R(r)$  for all  $q$ . In the range of  $r/\bar{\eta} > 200$  (containing ICR),  $\zeta_q^R(r)$  curves have a local maximum whose value is smaller than that of normal scaling  $\zeta_q = q/3$  evaluated by the dimensional arguments, whereas the curves of  $\zeta_q^G(r)$  decay as  $r$  increases further.

Possible reasons for the significant discrepancy of scaling behavior, especially at  $q > 4$ , from VCPR to ICR are (1) due to the insufficient time average, (2) to finite Reynolds number effects, and (3) to persistent anisotropy which is not

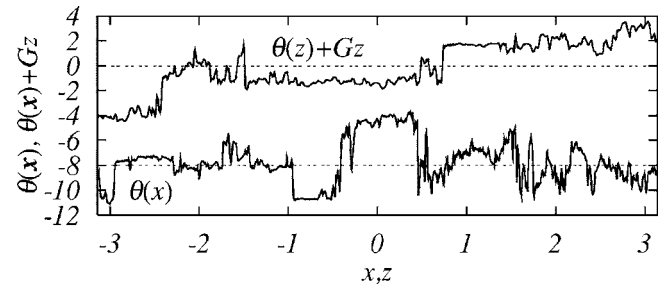
FIG. 3. Variation of  $\zeta_q^R(r)$  and  $\zeta_q^G(r)$  against  $R_\lambda$  for  $q=4$ .

fully eliminated by the simple procedure used in the present study.

As for reason (1), there is a possibility that the variation of instantaneous scaling exponent is affected by the creation and annihilation of fronts, where the frequency of their creation is controlled by the large eddy turnover time. Although our experience tells us that a couple of large eddy turnover time is not insufficient for evaluating the scaling exponent, the time average smoothing out such events may be more desirable to ensure the accuracy of scaling exponents.

For reasons (2) and (3), it is difficult to discuss the two effects individually. Comparison of the present results with those at approximately  $R_\lambda=260$  for cases  $R^{14}$  and  $G$  shows that when  $R_\lambda$  increases the local maximum of  $\zeta_4^R(r)$  in ICR moves toward larger  $r$  and decreases very slightly, whereas the horizontal part of the  $\zeta_4^G(r)$  curve in VCPR remains unchanged and slowly extends toward ICR, as seen in Fig. 3. There is no trend that the difference  $|\zeta_4^R(r) - \zeta_4^G(r)|$  becomes appreciably small for  $r/\etā > 100$ . As seen in the inset of Fig. 1 the difference  $\zeta_q^\perp(r) - \zeta_q^\parallel(r)$  is a measure of the anisotropy effects on the scaling exponents, and is very small in the range  $60 < r/\etā < 200$  even at  $q=8$ , meaning that the anisotropy effects are small in this range. The scaling behavior of isotropic and anisotropic sectors certainly needs further examination by the  $SO(3)$  decomposition of scalar structure function.<sup>18</sup> This issue is beyond the scope of the present study. One may draw a few possibilities such that when  $R_\lambda$  is very high (a) the local maximum of  $\zeta_4^R(r)$  attains a constant and its plateau extends large  $r$  and  $\zeta_4^G(r)$  gradually approaches  $\zeta_4^R(r)$  from small  $r$ , or (b) the curve  $\zeta_4^G(r)$  extends toward large  $r$  and  $\zeta_4^R(r)$  approaches  $\zeta_4^G(r)$ . It is not possible and useful to draw any definite statements from these data. We do not discuss it here and have to wait more reliable data.

Figure 4 shows the one-dimensional profiles of the scalar amplitude along  $\mathbf{e}_\parallel$  and  $\mathbf{e}_\perp$ . We can observe the plateaus in  $\theta(z) + Gz$ , i.e., the ramp structure. Length of the ramp is about the integral scale  $L$  ( $\approx 1.2$ ). Large jumps in  $\theta$  at cliffs are of the order of  $\theta_{rms}$  ( $\equiv \langle \theta^2 \rangle^{1/2}$ ). On the other hand, the field structure of  $\theta$  in  $\mathbf{e}_\perp$  direction is different, mesa and canyon<sup>14</sup> rather than ramp-cliff prevails. This difference is characterized by the statistics of derivative field  $\nabla\theta$ , where the skewness factor of  $\nabla_\parallel\theta$  is 1.15, whereas that of  $\nabla_\perp\theta$  is almost zero.

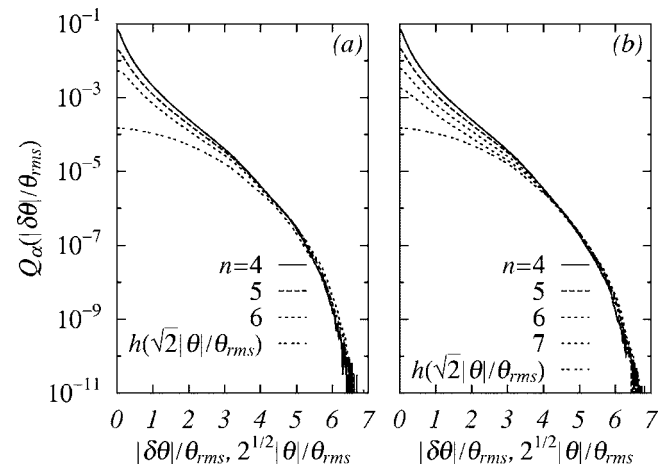
FIG. 4. One-dimensional profile of  $\theta + Gz$  (upper) and  $\theta$  (lower) along the directions of  $\mathbf{e}_\parallel$  and  $\mathbf{e}_\perp$  obtained from case  $G$ , respectively. The lower curve is shifted by  $-8$  for clarity. Horizontal dot lines denote the zero levels.

Saturation of the scaling exponents at high order implies that the probability density function (PDF)  $P_\alpha(\delta\theta, r)$  for  $|\delta\theta| \gg \sigma_{\delta\theta}$  is asymptotically

$$P_\alpha(\delta\theta, r) = \theta_{rms}^{-1} \left( \frac{r}{\etā} \right)^{\zeta_\infty^\alpha} Q_\alpha \left( \frac{\delta\theta}{\theta_{rms}} \right), \quad (1)$$

where  $Q_\alpha(x)$  is a function independent of  $r$ . Figure 5 shows plots of  $P_\alpha(|\delta\theta|, r)$  in terms of the scaling (1) with  $\zeta_\infty^\alpha=1.3$  for  $r=2^n\pi/N$  with  $n=4, \dots, 7$  which are within the plateau range of  $\zeta_q^\alpha(r)$  in Fig. 1. Curves collapse excellently over about five decades in magnitudes for  $|\delta\theta| > 4\theta_{rms}$ . The scaling law (1) has also been confirmed in VCPR of case  $R$  (but  $\zeta_\infty \approx 1.5$ ),<sup>14</sup> in the DNS of 2D passive scalar,<sup>5,6</sup> and in the measurement of temperature fluctuations for the low temperature helium experiment.<sup>19</sup>

As  $\theta$  is a *passive* scalar and there is no mechanism to self-amplify unlike the vorticity, the upper bound of the scalar increment is roughly estimated as  $|\delta_\alpha\theta_r| \sim \langle (\delta_\alpha\theta_L)^2 \rangle^{1/2} \approx \sqrt{2}\theta_{rms}$  irrespective of  $r$  because it is dominated by the large jump of  $\theta$  (cliff). Then the far tail of  $P_\alpha(\delta\theta)$  could be represented in terms of the one point PDF  $P(\theta)$  of  $\theta$  multiplied by the probability to find a cliff in the separation  $r$  as

FIG. 5. Scaling plots (1) with  $\zeta_\infty^\alpha=1.3$  for the PDFs of (a)  $|\delta_\parallel\theta_r|$  and (b)  $|\delta_\perp\theta_r|$ , respectively. Curve  $h(x)$  extracted from  $P(\theta)$  is also plotted to examine the relation (2).

$$P_\alpha(|\delta\theta|, r) \approx \frac{1}{\sqrt{2}} P\left(\frac{|\delta\theta|}{\sqrt{2}}\right) \left(\frac{r}{L}\right)^{\zeta_\infty^\alpha}. \quad (2)$$

The previous relation is examined in Fig. 5. The curves of  $Q_\alpha(x)$  and  $h(x) = (\theta_{\text{rms}}/\sqrt{2})(\bar{\eta}/L)^{\zeta_\infty^\alpha} P(\theta_{\text{rms}}x/\sqrt{2})$ , with  $\zeta_\infty^\alpha = 1.3$  agree quite satisfactorily in the range  $|\delta\theta| > 4\theta_{\text{rms}}$ . This means that the rare events at small scales are closely related to the large scale nature of the scalar field. Another point is that the tail of  $P_\alpha(|\delta\theta|, r)$  decays much faster than the Gaussian, which implies that the PDF tail of  $|\delta_\alpha\theta_r|$  is bounded.<sup>6,20</sup>

Relation (2) is important to understand the relation between the ramp-cliff structure and the saturation phenomenon. Suppose that the scalar increment  $|\delta_\alpha\theta_r|$  is expressed in terms of an exponent  $z$  which fluctuates in space and time and of the scalar amplitude  $|\theta|$  as  $|\delta_\alpha\theta_r| \sim \sqrt{2}|\theta|(L/r)^z$  with  $z \leq 0$ . Saturation of the scaling exponents at high order means  $|z| \ll 1$  and  $|\theta| > \theta_{\text{rms}}$ . Then the tail of  $P_\alpha(|\delta\theta|, r)$  is governed by that of  $P(|\theta|)$ . How is this realized? When the cliff is very sharp and resides in small regions, the scalar increment between two points encompassing the cliff is given by the jump in  $\theta$  of the order of  $\theta_{\text{rms}}$  and independent of the separation distance, meaning  $z \approx 0$ . Then the average of high order power of the scalar increment is determined by the geometrical dimension  $\mu$  of the spatial support of the cliff.<sup>6</sup> As the velocity field is isotropic in our cases  $R$  and  $G$ , it is quite reasonable to expect that the cliff is also isotropically distributed. Then we have  $\zeta_\infty^\alpha = 3 - \mu$ , meaning that the exponents are independent of  $\alpha$ . We roughly estimate  $\mu = 3 - \zeta_\infty^\alpha \approx 1.7$  from Fig. 2, which suggests that a geometry of the cliff set in 3D is between sheet and line. These arguments are speculative and numerical examination is necessary.

We infer that the saturation of the scaling exponents  $\zeta_q^||$  and  $\zeta_q^\perp$  at the high order is universal. However, the scaling exponents are dependent on scalar injection scheme at large scales within the Reynolds numbers studied. Present DNS study suggests that the examination of the universality of the passive scalar requires much larger Reynolds numbers than needed in the velocity case. Extrapolation from the existing theories and numerical or experimental data should be carefully made. Further study with very high resolution DNS is certainly indispensable.

The authors thank the Earth Simulator Center, the Theory and Computer Simulation Center of the National Institute for Fusion Science, and the Information Technology

Center of Nagoya University for providing the computational resources. One of the authors (T.W.) is supported by the Grant-in-Aid for Scientific Research No. 17760139 in the Ministry of Education, Culture, Sports, Science and Technology of Japan.

- <sup>1</sup>Z. Warhaft, "Passive scalars in turbulent flows," *Annu. Rev. Fluid Mech.* **32**, 203 (2000).
- <sup>2</sup>B. I. Shraiman and E. D. Siggia, "Scalar turbulence," *Nature (London)* **405**, 639 (2000).
- <sup>3</sup>G. Falkovich, K. Gawedzki, and M. Vergassola, "Particles and fields in fluid turbulence," *Rev. Mod. Phys.* **73**, 913 (2001).
- <sup>4</sup>A. Gylfason and Z. Warhaft, "On higher order passive scalar structure functions in grid turbulence," *Phys. Fluids* **16**, 4012 (2004).
- <sup>5</sup>A. Celani, A. Lanotte, A. Mazzino, and M. Vergassola, "Universality and saturation of intermittency in passive scalar turbulence," *Phys. Rev. Lett.* **84**, 2385 (2000).
- <sup>6</sup>A. Celani, A. Lanotte, A. Mazzino, and M. Vergassola, "Fronts in passive scalar turbulence," *Phys. Fluids* **13**, 1768 (2001).
- <sup>7</sup>R. H. Kraichnan, "Anomalous scaling of a randomly advected passive scalar," *Phys. Rev. Lett.* **72**, 1016 (1994).
- <sup>8</sup>M. Chertkov, G. Falkovich, I. Kolokolov, and V. Lebedev, "Normal and anomalous scaling of the fourth-order correlation function of a randomly advected passive scalar," *Phys. Rev. E* **52**, 4924 (1995).
- <sup>9</sup>K. Gawedzki and A. Kupiainen, "Anomalous scaling of the passive scalar," *Phys. Rev. Lett.* **75**, 3834 (1995).
- <sup>10</sup>I. Arad, L. Biferale, A. Celani, I. Procaccia, and M. Vergassola, "Statistical conservation laws in turbulent transport," *Phys. Rev. Lett.* **87**, 164502 (2001).
- <sup>11</sup>A. Celani and M. Vergassola, "Statistical geometry in scalar turbulence," *Phys. Rev. Lett.* **86**, 424 (2001).
- <sup>12</sup>T. Gotoh and T. Watanabe, "Statistics of transfer fluxes of the kinetic energy and scalar variance," *J. Turbul.* **6**, N33 (2005).
- <sup>13</sup>T. Gotoh, D. Fukayama, and T. Nakano, "Velocity field statistics in homogeneous steady turbulence obtained using a high-resolution direct numerical simulation," *Phys. Fluids* **14**, 1065 (2002).
- <sup>14</sup>T. Watanabe and T. Gotoh, "Statistics of a passive scalar in homogeneous turbulence," *New J. Phys.* **6**, 40 (2004).
- <sup>15</sup>P. K. Yeung, D. A. Donzis, and K. R. Sreenivasan, "High-Reynolds-number simulation of turbulent mixing," *Phys. Fluids* **17**, 081703 (2005).
- <sup>16</sup>T. Watanabe and T. Gotoh, "Intermittency, field structure and accuracy of DNS in a passive scalar turbulence," in *Proceedings of IUTAM Symposium on Elementary Vortices and Coherent Structures: Significance in Turbulence Dynamics*, edited by S. Kida (Springer, New York, 2006), pp. 171–176.
- <sup>17</sup>A. M. Yaglom, "On the local structure of a temperature field in a turbulent flow," *Dokl. Akad. Nauk Arm. SSR* **69**, 743 (1949).
- <sup>18</sup>L. Biferale and I. Procaccia, "Anisotropy in turbulent flows and in turbulent transport," *Phys. Rep.* **414**, 43 (2005).
- <sup>19</sup>F. Moisy, H. Willaime, J. S. Andersen, and P. Tabeling, "Passive scalar intermittency in low temperature helium flows," *Phys. Rev. Lett.* **86**, 4827 (2001).
- <sup>20</sup>A. Noullez, G. Wallace, W. Lempert, R. B. Miles, and U. Frisch, "Transverse velocity increments in turbulent flow using the RELIEF technique," *J. Fluid Mech.* **339**, 287 (1997).